Transcranial Doppler-derived indices of cerebrovascular haemodynamics are independent of depth and angle of insonation

Michael Heckelmann [a], Ganeshwaran Shivapathasundram [a], Danilo Cardim [b], Peter Smielewski [b], Marek Czosnyka [b], Rita Gaio [c], Mark M. P. Sheridan [a,d], Matthias Jaeger [d,e,f]

[a] *Department of Neurosurgery, Liverpool Hospital, Liverpool, NSW, Australia.*

[b] *Department of Clinical Neurosciences, Neurosurgical Unit, University of Cambridge, Addenbrooke's Hospital, Cambridge, United Kingdom.*

[c] *Department of Mathematics, Faculty of Sciences, University of Porto and Centre of Mathematics of the University of Porto, Porto, Portugal.*

[d] *University of New South Wales, South Western Sydney Clinical School, Liverpool, NSW, Australia.*

[e] *Illawarra Health and Medical Research Institute, Wollongong, NSW, Australia.*

[f] *Department of Neurosurgery, Wollongong Hospital, Wollongong, NSW, Australia.*

Corresponding author:
Michael Heckelmann
heckelmann.michael@gmail.com
Phone: +61 (0)411 205 543
Present address:
602/19 Holdfast Promenade
Glenelg 5045, SA, Australia

ABSTRACT

Continuous measurement of cerebral blood flow velocity (CBFV) of the middle cerebral artery (MCA) using transcranial Doppler (TCD) and arterial blood pressure (ABP) monitoring enables assessment of cerebrovascular haemodynamics. Further indices describing cerebrovascular function can be calculated from ABP and CBFV, such as the mean index (Mxa) of cerebrovascular autoregulation, the 'time constant of the cerebral arterial bed' (*tau*), the 'critical closing pressure' (CrCP) and a 'non-invasive estimator of ICP' (nICP). However, TCD is operator-dependent and changes in angle and depth of MCA insonation result in different readings of CBFV. The effect of differing CBFV readings on the calculated secondary indices remains unknown. The aim of this study was to investigate variation in angle and depth of MCA insonation on these secondary indices. In eight patients continuous ABP and ipsilateral CBFV monitoring was performed using two different TCD probes, resulting in four simultaneous CBFV readings at different angles and depths per patient. From all individual recordings, the K-means clustering algorithm was applied to the four simultaneous longitudinal measurements. The average ratios of the between-clusters, sum-of-squares and total sum-of-squares were significantly higher for CBFV than for the indices Mxa, *tau* and CrCP ($p<0.001$, $p=0.007$ and $p=0.016$) but not for nICP ($p=0.175$). The results indicate that Mxa, *tau* and CrCP seemed to be not affected by depth and angle of TCD insonation, whereas nICP was.

Key words (MeSH terms)

Ultrasonography; Transcranial Doppler; Cerebral Autoregulation; Monitoring; Mean index.

1. Introduction

Transcranial Doppler ultrasonography (TCD) has developed into a widespread and diversely used tool in neurological diagnostics and brain-neurocritical care[1-6] since its first description in 1982 by Aaslid et al. [7]. Especially TCD of the middle cerebral artery (MCA), monitoring cerebral blood flow velocity (CBFV), has established as a non-invasive instrument to assess multiple properties and aspects of cerebrovascular haemodynamics [8,9] in the setting of neuromonitoring. The TCD-derived mean index of cerebral autoregulation (Mxa) has prognostic significance in a number of acute conditions relevant to neurocritical care, such as traumatic brain injury, aneurysmal subarachnoid haemorrhage and stroke [10-12]. Other relevant parameters of cerebrovascular function obtained from TCD are the critical closing pressure (CrCP) of the cerebral circulation [13-16], the time constant of the cerebral arterial bed (τ *or tau)* [17-19] and the non-invasive estimator of ICP (nICP) [20]. These indices were selected for this study as they are based on continuous TCD readings and do not require external stimulation or manipulation of the patient's cardiovascular system to test or monitor cerebrovascular function or autoregulation. In this respect they are suitable to investigate the influence of insonation of TCD reading on their values.

One of the main advantages of TCD for monitoring these various indices of cerebrovascular function is its non-invasive technique, as compared to invasive methods using surgically implanted probes to measure intracranial pressure or brain tissue oxygen. However, TCD is highly operator-dependent and the angle and depth of blood vessel insonation can significantly change the measured CBFV [21-23]. For example, slight variation in the position of a standard 2 MHz TCD probe only for a couple of millimetres on the patient's head, thus changing the angle of MCA insonation, can significantly

change the CBFV readings. Whilst investigators would typically aim to obtain the best TCD signal with a handheld probe, this can be more difficult when the TCD probe is mounted to a headframe, as commonly done for continuous TCD measurements over prolonged periods of time. It is unknown if this variation in CBFV readings due to probe position also affects the calculation of the TCD-derived parameters Mxa, CrCP, *tau* or nICP.

The aim of this study was to evaluate the effect of different angles and depths of MCA insonation on multiple TCD-derived parameters describing the function of the cerebral circulation. We investigated this by performing continuous synchronous ipsilateral CBFV recordings of the MCA using two adjacent TCD probes at two different depths of insonation each in patients with acute cerebral insults.

2. Methods

Eight patients were included in this study. Table 1 presents demographic information and clinical characteristics of these patients.

The ethics committee of South Western Sydney health district approved this study (HREC/12/LPOOL/110; SSA/12/LPOOL/205; project number 12/069). Written informed consent was obtained from the next of kin. All patients required sedation and artificial ventilation due to injury severity and were treated according to accepted disease specific clinical standards.

2.1. Monitoring of cerebral blood flow velocity and arterial blood pressure

Arterial blood pressure (ABP) was continuously monitored through an arterial line in the radial artery as part of routine management. Two TCD probes (DWL Compumedics, Singen, Germany) were mounted unilaterally on a head frame to monitor CBFV of the MCA simultaneously at two separate insonation angles (Figure 1). Each probe allowed measurement at two different depths simultaneously, thus four synchronous TCD readings were available per patient. We typically aimed for depths of measurement of 45 mm and 55 mm with each probe. The probes were adjusted and fixed to a head frame to obtain the best possible and stable TCD signal for each of the four CBFV readings. ABP and the 4 CBFV signals were recorded at 200 Hz using ICM+ software (Cambridge Enterprise Ltd, UK). The duration of TCD monitoring per patient is given in table 1. The ABP and CBFV signals were then averaged over 10 s intervals for calculation of mean arterial pressure (MAP) and further parameters as described below.

2.2. Mean index (Mxa)

The Mxa-index was calculated as the moving Pearson's correlation coefficient between MAP and CBFV using a window of 300 seconds, thus incorporating 30 values of ABP and CBFV [10]. The window was updated every 30 seconds. Using this established method, the slow wave oscillations in cerebral heamodynamics are captured, which are assumed to carry information about autoregulatory capacity. CBFV and ABP data are averaged over 10-seconds to filter potential contaminants from the signal, such as respiratory waves. In addition, wide calculation windows may introduce additional confounds during the monitoring period, such as movements, nursing manoeuvres or drug

96 administration. As such, 10-second averaged values for 300-second durations (5-minutes
97 period or 0.003 Hz characteristic of slow waves incidence) are used to integrate
98 approximately 30 data points for each Mxa calculation before the window moves 30-
99 seconds forward (update period) in time and repeats the calculation to avoid the potential
100 confounders mentioned.
101
102
103 *2.3. 'Non-invasive estimator of ICP' (nICP)*
104 nICP was calculated using a mathematical black-box model [20,24], in which the
105 intracranial compartment was considered a black-box system. This mathematical model
106 is based on results from systems analysis, which provides a method to describe systems,
107 in particular physiological systems, with input and output signals. The outgoing signals
108 are considered the system's responses to its stimulation by incoming signals. In this case,
109 the intracranial compartment was indirectly described by a transfer function approach
110 [25,26] which connected the assumed input signal ABP with the output signal ICP (nICP).
111 The transformation rules between ABP and ICP were controlled and continuously
112 adjusted by selected hemodynamic parameters (TCD-characteristics), characterising
113 patterns of CBFV as well as the ABP-CBFV relationship. A constant relationship between
114 CBFV-ABP and ABP-nICP transformations was derived from analysis of a database
115 including 140 traumatic brain injury (TBI) patients [7]. For this nICP model, the transfer
116 function between ABP and ICP (unknown transfer function) was dynamically controlled
117 by TCD and ABP derived parameters, the so-called TCD characteristics, which included
118 ICP-related parameters and an ABP to TCD transfer function (a known transfer function).
119 The rules of this TCD-based linear control had been formerly determined using a multiple

120 regression model between TCD characteristics and ABP-ICP transfer function on datasets
121 of reference patients [7]. Non-invasive ICP estimation using this method was performed
122 using a plugin developed for ICM+ software [27].
123
124
125 *2.4. 'Time Constant of the Cerebral Arterial Bed' (τ* or *tau)*
126 The Time Constant of Cerebral Arterial Bed (τ) was calculated from ABP and CBFV
127 as described by Kasprowicz *et al.* [17-19]:

128 $$\tau = C_a \times CVR = \frac{Amp_{C_aBV} \times S_a}{Amp_{ABP}} \times \frac{meanABP}{meanCBFV \times S_a} \quad [s]$$

129 , where C_a is the compliance of the arterial bed, estimated using:

130 $$C_a = \frac{AMP_{C_aBV} \times S_a}{Amp_{ABP}} \qquad \left[\frac{cm^2 \times \frac{cm}{s} \times s}{mmHg}\right]$$

131 , CVR is the cerebrovascular resistance, approximated using:

132 $$CVR = \frac{meanABP}{meanCBFV \times S_a} \qquad \left[\frac{mmHg}{\frac{cm}{s} \times cm^2}\right]$$

133 In these formulae Amp_{ABP} is the first harmonic amplitude of arterial blood pressure pulse
134 waveform and AMP_{CaBV} is the first harmonic amplitude of the blood volume pulse
135 waveform, the latter calculated as an integral of the FV signal.
136 The unknown cross-sectional area of the arterial vessel (S_a) cancels out in the formula for
137 τ.
138

139

140 *2.5. The Critical Closing Pressure (CrCP)*

141 As described in detail by Varsos *et al.* [14-16] CrCP was estimated noninvasively on
142 the basis of the digitally recorded values of ABP and CBFV using the equation:

$$CrCp = ABP \times \left[1 - \frac{1}{\sqrt{\left(CVR \times Ca \times HR \times 2\pi\right)^2 + 1}}\right]$$

143

144 in which HR represents the heart rate, Ca stands for the compliance of the arterial bed
145 and CVR for cerebrovascular resistance (Ca and CVR were calculated as above).

146

147

148 *2.6. Statistical methods*

149 Prior to statistical analysis all data was prepared by averaging of the values obtained
150 for each 300s periods across the monitoring time.

151 The aim of the statistical analysis was to investigate if the secondary indices of
152 cerebral haemodynamics and autoregulation are robust enough to cope with an undefined
153 deviation in angle and depth of insonation in TCD, based on the four simultaneous sets
154 of data recordings obtained for each of the eight patients.

155 The acquired longitudinal data for comparison consisted of measurements in the
156 same individual over time, denoted by trajectories, under different conditions (differing
157 in an undefined manner in angle and depth of insonation).

158 For each studied index, each patient presented 4 trajectories that eventually could be
159 grouped into two pairs (of trajectories) but the pairing itself was unknown - the pairing
160 resembling the data collection with two different ultrasound probes. We therefore applied
161 a longitudinal K-means algorithm (KmL) [28,29] to each index and to each patient, with

the choice of two clusters, thus performing a similar procedure 40 times (8 patients, 5 indices). In each procedure, the algorithm was run 100 times, with randomly chosen starting conditions, in order to ensure convergence of the algorithm and robustness of results.

For each of the 40 obtained cluster structures the ratio between the between-clusters sum-of-squares (BSS) and the total sum-of-squares (TSS) was computed and the obtained 40 values were plotted for visualization (see Results, Figure 2). In our context, for patient i (i=1,2,…,8), index v (v=1,2,…,5), time t (t=1,2,…,T_i), modality of insonation l (l=1,2,3,4) and cluster k (k=1,2), TSS_{iv} and BSS_{iv} correspond to

$$TSS_{iv} = \sum_{l=1}^{4} \sum_{t=1}^{T_i} (y_{ltiv} - \bar{y}_{tiv})^2$$

and

$$BSS_{iv} = 2 \sum_{k=1}^{2} \sum_{t=1}^{T_i} (\bar{y}_{ktiv} - \bar{y}_{tiv})^2$$

where $\bar{y}_{tiv}$ represents the average over the four modalities and $\bar{y}_{ktiv}$ stands for the average over the two modalities of cluster k and T_i is the number of measurements of index v for patient i. The factor 2 in the formula for BSS_{iv} is due to the fact that each cluster consists of two trajectories.

The ratio BSS/TSS takes values between 0 and 1 and reflects the percentage of total variation that is explained by the clusters' structure, which can be thought of as a quality index of the clustering. The closer the ratio is to 1, the better. Differences between the means of the ratios across the indices were evaluated by Tukey's multiple comparison test after 1-way repeated measures ANOVA.

The comparison of the behaviour of CBFV within each mean cluster curve and the investigation of the effect of CBFV on Mxa were evaluated by mixed-effects regression models. The intra-individual variability was taken into account by a random intercept and temporal dependencies were integrated into an autoregressive residuals correlation structure of order 1. Comparison between models was based on the likelihood ratio test for nested models and on the Akaike Information Criteria (AIC) [30] otherwise. Table 2 summarises the statistical results.

Statistical analyses were carried out using the R language and software environment for statistical computation, version 3.6.3 [31]. The significance level was set at 0.05.

3. Results

3.1. Primary acquired data and resulting secondary indices

An overview of the primarily recorded measurements, averaged over the whole period of the recording for each patient are provided in table 3. These demonstrate that the synchronously acquired intraindividual CBFV measurements 1-4 diverge markedly. Table 4 shows the values of Mxa, CrCP, *tau* and nICP for each patient.

3.2. Statistical comparison of the synchronous measurements and derived indices demonstrates that the secondary indices Mxa, tau, CrCP are not influenced by the modality of insonation

As required, the longitudinal clustering algorithm identified two cluster curves (pairings) within each individual and index. The average (across patients) ratio BSS/TSS was significantly higher for CBFV than for all the remaining indices but nICP ($p<0.001$,

p=0.007, p=0.016 and p=0.175 for comparisons with Mxa, *tau*, CrCP and nICP, respectively), meaning that among all studied indices, CBFV and nICP were those that best identified the two pairings of the four modalities of insonation. Figure 2 shows the clustering index BSS/TSS for CBFV and the secondary indices. On the other hand, Mxa was the index with the lowest average ratio BSS/TSS (comparison of Mxa with *tau, CrCP and nICP:* p=0.935, p=0.845 and p=0.308, respectively), only significantly different from CBFV ($p<0.001$). Thus, CBFV is the index that best identifies the two cluster curves.

Moreover, a mixed-effects regression model controlling for intra-individual variation at the intercept showed that the 2-cluster curves presented longitudinal significantly different profiles for CBFV (p=0.031). Hence, the two mean cluster curves for CBFV are significantly different from one another.

A concurrent result to what is being reported is the fact that CBFV also did not have a significant effect on Mxa (p=0.206).

Figure 3 demonstrates the plots of the TCD-derived CBFV and the secondary indices.

4. Discussion

This study analysed the effects of different angles and depths of TCD insonation of the MCA on the readings of CBFV and derived indices of cerebrovascular function Mxa, *tau*, CrCP and nICP in a small cohort of patients with acute cerebral insults.

While there are several other indices established to test and monitor cerebrovascular function and autoregulation, these four indices were selected because they allow to investigate the influence of TCD insonation characteristics. Other indices, as the ‘pressure

reactivity index' (PRx), the 'mean flow velocity index' (Mx-CPP) or the 'dynamic autoregulation index' (ARI), have been found to demonstrated higher clinical significance [32], but they are either based on invasive ICP readings to provide CPP data in case of PRx and Mx-CPP or require stimulation of the cardiovascular system as ARI. As such, these indices, as several others, were not applicable for this investigation despite higher clinical potential.

We found significant differences in CBFV within individuals from the four different synchronous TCD readings. Interestingly, this did not influence the autoregulation index Mxa, which was not statistically different between the four readings. The results of the statistical analysis suggest that, despite the significant influence of the method of reading CBFV by TCD, using different angle and depth, on the mean values, the calculated secondary indices seemed to be much less affected. The analysis of the 2-cluster curves demonstrated a significantly different behaviour of CBFV compared to the curves of the secondary indices Mxa, CrCP and tau(τ). This might indicate that Mxa, *tau* (τ) and CrCP are quite robust parameters for potential bedside use; as long as the TCD probe is stable in its position while reading of MCA CBFV, angle and depth will not affect their calculation.

The autoregulatory function measured by Mxa is mainly based on the stimulus of the slow waves of ABP and the resultant CBFV slow wave response. It appears that this cerebrovascular response can be measured relatively independent of the angle and depth of TCD insonation. Interestingly, the calculations of nICP derived from TCD and ABP using the black box model did not demonstrate to be independent from insonation conditions. This would indicate that contrary to the other indices analyzed in this study,

optimal insonation conditions are more crucial when non-invasive ICP is derived from TCD. This might be a technical and methodical aspect of the issues with reliability and accuracy that have been found with non-invasive monitoring of ICP [33] however given the relatively high 95% confidence interval for this parameter (±10 mmHg or more) one cannot really make firm conclusion as to robustness of it in this small cohort.

The main limitation of our study is the small sample size of n = 8 prospectively enrolled patients. However, it might serve as a pilot study leading to future work with larger numbers. As CBFV and autoregulation can be influenced by other factors, for example CO_2 [34], these parameters, that were not document in this study, might improve the analysis of the influence of TCD insonation.

The authors are not aware of other studies comparing the effects of different angles and depths of insonation on monitoring of cerebral autoregulation and other indices of cerebrovascular function. This study might help to elucidate a knowledge gap about reliability of using TCD-derived measures in neuromonitoring.

5. Conclusion

Our pilot study showed that the mean index of cerebral autoregulation, Mxa, is likely not significantly affected by the depth and angle of TCD insonation. This also accounts for the cerebrovascular indices CrCP and *tau*. Hence, despite inter-operator variability in measuring CBFV by TCD, this non-invasive method can be used to calculate and monitor these indices of cerebrovascular function. Robustness of nICP to the TCD insonation conditions was inconclusive and requires further investigation.

Acknowledgments

RG was partially supported by CMUP (UID/MAT/00144/2013), which is funded by FCT (Portugal) with national (MEC) and European structural funds (FEDER), under the partnership agreement PT2020.

MC was supported by NIHR Medical Informatics Cooperative. PS and MC have interest in a part of ICM+ software licensing fee (Cambridge Enterprise Ltd, UK)

References

[1] Robba C, Cardim D, Sekhon M, Budohoski K, Czosnyka M. Transcranial Doppler: a stethoscope for the brain-neurocritical care use. J Neuro Res 2017;96:720–30. doi:10.1002/jnr.24148.

[2] Laumer R, Steinmeier R, Gönner F, Vogtmann T, Priem R, Fahlbusch R. Cerebral hemodynamics in subarachnoid hemorrhage evaluated by transcranial Doppler sonography. Part 1. Reliability of flow velocities in clinical management. Neurosurgery 1993;33:1–8–discussion8–9. doi:10.1227/00006123-199307000-00001.

[3] Steinmeier R, Laumer R, Bondár I, Priem R, Fahlbusch R. Cerebral hemodynamics in subarachnoid hemorrhage evaluated by transcranial Doppler sonography. Part 2. Pulsatility indices: normal reference values and characteristics in subarachnoid hemorrhage. Neurosurgery 1993;33:10–8–discussion18–9. doi:10.1227/00006123-199307000-00002.

[4] Hartl WH, Fürst H. Application of Transcranial Doppler Sonography to Evaluate Cerebral Hemodynamics in Carotid Artery Disease. Stroke 1995;26:2293–7. doi:10.1161/01.STR.26.12.2293.

[5] Elzaafarany K, Aly MH, Kumar G, Nakhmani A. Cerebral Artery Vasospasm Detection Using Transcranial Doppler Signal Analysis. J Ultrasound Med 2019;38:2191–202. doi:10.1002/jum.14916.

[6] Azevedo DS, Salinet ASM, Oliveira M, Teixeira MJ, Bor-Seng-Shu E, Nogueira R. Cerebral hemodynamics in sepsis assessed by transcranial Doppler: a systematic review and meta-analysis. Journal of Clinical Monitoring and Computing 2016;31:1123–32. doi:10.1007/s10877-016-9945-2.

[7] Aaslid R, Markwalder TM, Nornes H. Noninvasive transcranial Doppler ultrasound recording of flow velocity in basal cerebral arteries 1982;57:769–74. doi:10.3171/jns.1982.57.6.0769.

[8] Birch AA, Dirnhuber MJ, Hartley-Davies R, Iannotti F, Neil-Dwyer G. Assessment of autoregulation by means of periodic changes in blood pressure. Stroke 1995;26:834–7. doi:10.1161/01.str.26.5.834.

[9] Czosnyka M, Brady K, Reinhard M, Smielewski P, Steiner LA. Monitoring of cerebrovascular autoregulation: facts, myths, and missing links. Neurocrit Care 2009;10:373–86. doi:10.1007/s12028-008-9175-7.

[10] Czosnyka M, Smielewski P, Kirkpatrick P, Menon DK, Pickard JD. Monitoring of cerebral autoregulation in head-injured patients. Stroke 1996;27:1829–34. doi:10.1161/01.str.27.10.1829.

[11] Soehle M, Czosnyka M, Pickard JD, Kirkpatrick PJ. Continuous assessment of cerebral autoregulation in subarachnoid hemorrhage. Anesthesia & Analgesia 2004;98:1133–9–tableofcontents. doi:10.1213/01.ane.0000111101.41190.99.

[12] Xiong L, Liu X, Shang T, Smielewski P, Donnelly J, Guo Z-N, et al. Impaired cerebral autoregulation: measurement and application to stroke. Journal of Neurology, Neurosurgery & Psychiatry 2017;88:520–31. doi:10.1136/jnnp-2016-314385.

[13] Burton AC. On the physical equilibrium of small blood vessels. Am J Physiol 1951;164:319–29.

[14] Varsos GV, Kolias AG, Smielewski P, Brady KM, Varsos VG, Hutchinson PJ, et al. A noninvasive estimation of cerebral perfusion pressure using critical

closing pressure. Journal of Neurosurgery 2015;123:638–48. doi:10.3171/2014.10.JNS14613.
[15] Varsos GV, Richards H, Kasprowicz M, Budohoski KP, Brady KM, Reinhard M, et al. Critical closing pressure determined with a model of cerebrovascular impedance. Journal of Cerebral Blood Flow &Amp; Metabolism 2012;33:235–43. doi:10.1038/jcbfm.2012.161.
[16] Varsos GV, Budohoski KP, Czosnyka M, Kolias AG, Nasr N, Donnelly J, et al. Cerebral vasospasm affects arterial critical closing pressure. Journal of Cerebral Blood Flow &Amp; Metabolism 2014;35:285–91. doi:10.1038/jcbfm.2014.198.
[17] Kasprowicz M, Czosnyka M, Soehle M, Smielewski P, Kirkpatrick PJ, Pickard JD, et al. Vasospasm Shortens Cerebral Arterial Time Constant. Neurocrit Care 2011;16:213–8. doi:10.1007/s12028-011-9653-1.
[18] Kasprowicz M, Czosnyka M, Poplawska K, Reinhard M. Cerebral Arterial Time Constant Recorded from the MCA and PICA in Normal Subjects. Acta Neurochir Suppl 2016;122:211–4. doi:10.1007/978-3-319-22533-3_42.
[19] Kasprowicz M, Diedler J, Reinhard M, Carrera E, Smielewski P, Budohoski KP, et al. Time constant of the cerebral arterial bed. Acta Neurochir Suppl 2012;114:17–21. doi:10.1007/978-3-7091-0956-4_4.
[20] Schmidt B, Klingelhofer J, Schwarze JJ, Sander D, Wittich I. Noninvasive Prediction of Intracranial Pressure Curves Using Transcranial Doppler Ultrasonography and Blood Pressure Curves. Stroke 1997;28:2465–72. doi:10.1161/01.str.28.12.2465.
[21] Martin NA, Thomas KM, Caron M. Transcranial Doppler-Techniques, Application, and Instrumentation. Neurosurgery 1993;33:761–3. doi:10.1227/00006123-199310000-00033.
[22] Shen Q, Stuart J, Venkatesh B, Wallace J, Lipman J. Inter Observer Variability of the Transcranial Doppler Ultrasound Technique: Impact of Lack of Practice on the Accuracy of Measurement. Journal of Clinical Monitoring and Computing 1999;15:179–84. doi:10.1023/A:1009925811965.
[23] McMahon CJ, Mcdermott P, Horsfall D, Selvarajah JR, King AT, Vail A. The reproducibility of transcranial Doppler middle cerebral artery velocity measurements: Implications for clinical practice. Br J Neurosurg 2009;21:21–7. doi:10.1080/02688690701210539.
[24] Schmidt B, Czosnyka M, Schwarze JJ, Sander D, Gerstner W, Lumenta CB, et al. Cerebral vasodilatation causing acute intracranial hypertension: a method for noninvasive assessment. J Cereb Blood Flow Metab 1999;19:990–6. doi:10.1097/00004647-199909000-00006.
[25] Kasuga Y, Nagai H, Hasegawa Y, Nitta M. Transmission characteristics of pulse waves in the intracranial cavity of dogs. Journal of Neurosurgery 1987;66:907–14. doi:10.3171/jns.1987.66.6.0907.
[26] Marmarelis PZ, Marmarelis VZ. Analysis of Physiological Signals. Analysis of Physiological Systems, Boston, MA: Springer US; 1978, pp. 11–69. doi:10.1007/978-1-4613-3970-0_2.
[27] Czosnyka M, Matta BF, Smielewski P, Kirkpatrick PJ, Pickard JD. Cerebral perfusion pressure in head-injured patients: a noninvasive assessment using transcranial Doppler ultrasonography. Journal of Neurosurgery 1998;88:802–8. doi:10.3171/jns.1998.88.5.0802.

[28] Genolini C, Falissard B. KmL: k-means for longitudinal data. Comput Stat 2009;25:317–28. doi:10.1007/s00180-009-0178-4.
[29] Genolini C, Falissard B. KmL: a package to cluster longitudinal data. Comput Methods Programs Biomed 2011;104:e112–21. doi:10.1016/j.cmpb.2011.05.008.
[30] Akaike H. A New Look at the Statistical Model Identification. IEEE Trans Automat Contr 1974;19:716–23. doi:10.1109/TAC.1974.1100705.
[31] R Development Core Team. R: A Language and Environment for Statistical Computing. R Foundation for Statistical Computing, Vienna, Austria 2008.
[32] Rivera-Lara L, Zorrilla-Vaca A, Geocadin R, Ziai W, Healy R, Thompson R, et al. Predictors of Outcome With Cerebral Autoregulation Monitoring. Crit Care Med 2017;45:695–704. doi:10.1097/CCM.0000000000002251.
[33] Cardim D, Robba C, Bohdanowicz M, Donnelly J, Cabella B, Liu X, et al. Non-invasive Monitoring of Intracranial Pressure Using Transcranial Doppler Ultrasonography: Is It Possible? Neurocrit Care 2016;25:473–91. doi:10.1007/s12028-016-0258-6.
[34] Aries MJH, Elting JW, De Keyser J, Kremer BPH, Vroomen PCAJ. Cerebral Autoregulation in Stroke A Review of Transcranial Doppler Studies. Stroke 2010;41:2697–704. doi:10.1161/STROKEAHA.110.594168.
[35] Schwarz G. Estimating the Dimension of a Model. The Annals of Statistics 1978;6:461–4. doi:10.1214/aos/1176344136.

Table 1

Clinical characteristics of patients

No	Age	Sex	Insult	Duration of TCD measurement	GCS	GOS
1	58	f	SAH	41 min	15	3
2	44	m	TBI	49 min	13	4
3	26	m	TBI	38 min	7	5
4	50	m	TBI	16 min	3	4
5	63	f	ICH	27 min	11	5
6	35	m	TBI	39 min	5	2
7	83	f	TBI	34 min	11	1
8	68	m	SAH	84 min	8	2

SAH – aneurysmal subarachnoid haemorrhage, TBI traumatic brain injury, ICH – primary intracerebral hemorrhage, GCS Glasgow Coma Score, GOS Glasgow Outcome Score

Table 2

Summary of model fit for correlation between the observations within each individual.

Estimates from the linear mixed-effects model for CBFV. The residual standard error was estimated at 0.301. The model considered a correlation autoregressive structure of order 1 (AR(1), with a correlation coefficient estimated at 0.495)

AIC	BIC	logLik
64.5	81.1	27.3
Random effects:		StdDev
Residual		0.301
Correlation Structure: AR(1)		Phi
Parameter estimate(s)		0.495

	Fixed effects			**Random effects** (SD)
Variables	Estimate	Std Error	p-value	Intercept
Intercept	64.451	7.517	0.000	0.269
Cluster	3.913	1.800	0.031	

AIC Akaike Information Criterion (Akaike, 1974) [30]
BIC Bayesian Information Criterion (Schwarz, 1978) [35]
logLik Log-Likelihood – unpenalized goodness-of-fit measure.

Table 3

Average mean arterial pressure and cerebral blood flow velocities for each patient.

Patient	MAP [mmHg]	CBFV1 [cm/s]	CBFV2 [cm/s]	CBFV3 [cm/s]	CBFV4 [cm/s]
1	102.2	56.25	70.26	58.82	68.26
2	101.5	34.03	32.05	36.74	38.25
3	75.79	73.77	74.69	71.49	75.02
4	77.98	69.95	88.28	62.68	63.77

5	67.88	64.53	57.05	70.29	50
6	82.9	78.7	112	105	134
7	55.6	33.66	57.05	41.28	53.14
8	94.6	65.08	62.2	80.7	72.8

435
436
437 **Table 4**
438 Overview over the averaged
439 secondary indices Mxa and *tau* (**A**),
440 CrCP and nICP (**B**).
441
442
443 **A**

Patient	Mxa1	Mxa2	Mxa3	Mxa4	*tau*1	*tau*2 [s]	*tau*3	*tau*4
1	0.37	0.40	0.40	0.44	0.14	0.10	0.15	0.15
2	0.49	0.18	0.49	0.53	0.23	0.22	0.24	0.26
3	0.57	0.56	0.60	0.57	0.16	0.16	0.16	0.16
4	0.02	-0.03	-0.01	-0.10	0.09	0.09	0.09	0.09
5	0.56	0.71	0.76	0.56	0.30	0.28	0.30	0.28
6	0.30	0.15	0.18	0.11	0.17	0.18	0.18	0.17
7	0.97	0.95	0.92	0.84	0.23	0.28	0.25	0.28
8	0.22	0.17	0.24	0.23	0.19	0.19	0.21	0.21

444 **B**

Patient	CrCP1	CrCP2	CrCP3	CrCP4	nICP1	nICP2	nICP3	nICP4
	[mmHg]				[mmHg]			
1	29.20	26.35	29.59	31.17	14.63	16.73	17.85	18.23
2	36.90	36.57	38.73	41.51	9.39	8.25	12.59	9.80
3	36.81	37.29	35.99	37.40	15.53	15.96	14.67	16.01
4	24.22	25.56	23.87	23.50	12.31	13.55	12.44	11.78
5	33.86	32.57	33.69	31.77	15.53	14.14	16.36	14.61
6	33.37	33.89	35.17	33.30	17.40	18.56	18.91	18.50
7	32.90	36.07	34.30	36.29	17.19	20.78	21.47	24.65
8	34.92	35.50	38.22	39.36	17.75	17.30	20.61	20.59

445
446
447
448 **Fig. 1.** Illustration of the positioning of the transcranial Doppler ultrasound probes for continuous
449 monitoring, depicting reading of the middle cerebral artery through the temporal insonation
450 window: Two Doppler probes were mounted ipsilaterally in two different angles (**a**) and set to

obtain the cerebral blood flow velocity of the middle cerebral artery in two different depths (**b**) of insonation, thus recording four different measurements synchronously.

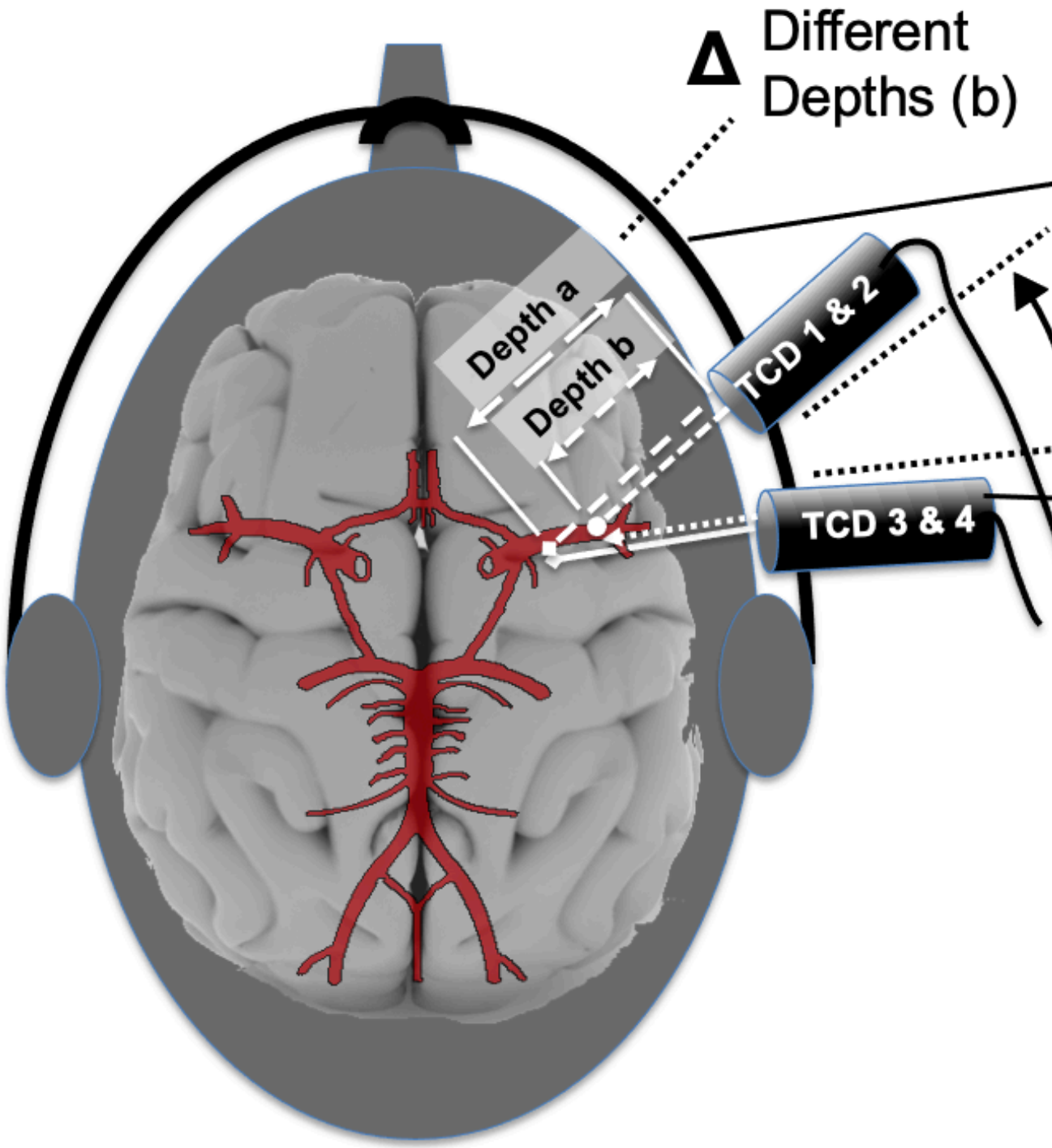

Fig. 2. Plots of the **Clusters' Variation Ratio** for **CBFV** and the secondary indices **Mxa**, **tau**, **CrCP** and **nICP**. Each symbol (⊠, +, ○, △, ▽, X, ✳, ◇) represents a patient. The same symbols were used across the indices. The clusters' variation ratio represents, for each patient and each index, the percentage of the total variation explained by the clusters' structure. It varies between 0 and 1, where closer to 1 means a higher identification with the 2-group structure within the four measurements.

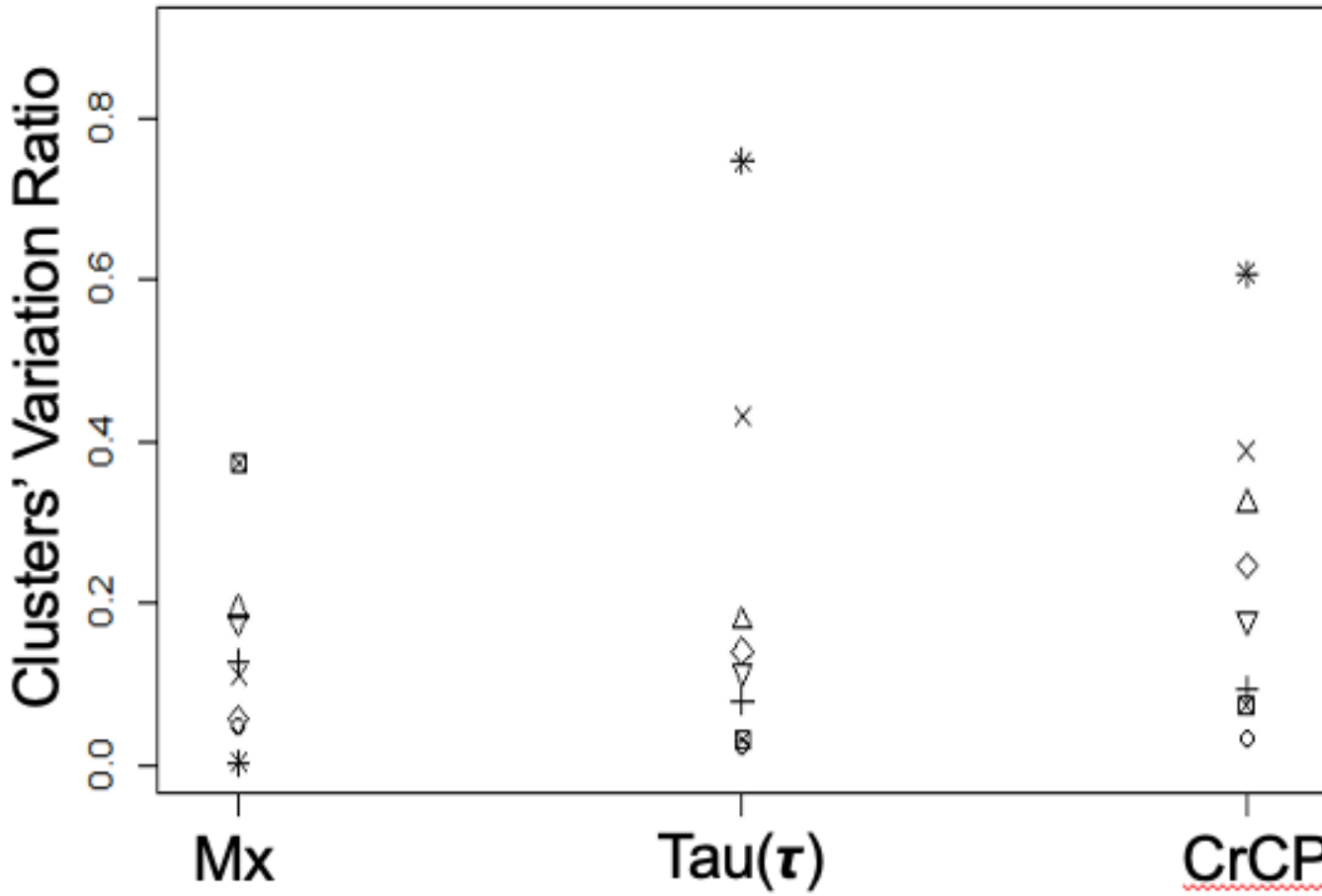

Fig. 3. Illustrative plots for CBFV (**A**) and the indices Mx (**B**), tau(τ) (**C**), CrCP (**D**) nICP (**E**) for one patient. A clustering algorithm was applied to the four simultaneous longitudinal measurements of each index: Measurement 1: squares (■) and solid lines; measurement 2: triangles (▲) and dotted lines; measurement 3: plus-signs (**+**) and dashed lines; measurement 4: circles (●) and dot-dashed lines.
The 2-cluster structure for CBFV(**A**) is obvious (measurements 2 & 3 versus measurements 1 & 4). While for the derived indices Mxa, tau and CrCP (**B-D**) that 2-cluster structure cannot be identified. The plots for nICP show a 2-cluster structure (**E**, 1&2 vs 3&4)

480
481